Science Journal of Chemistry
2022; 10(5): 144-151
http://www.sciencepublishinggroup.com/j/sjc
doi: 10.11648/j.sjc.20221005.12
ISSN: 2330-0981 (Print); ISSN: 2330-099X (Online)

Comparative Analysis of the Experimental, Computational, and Bacterial Growth Inhibition Studies on the Structure of N-Salicylidene Alanine Ni (II) Complex

James Tembei Titah[1, *], Tara Sheets[1], Liang Yang[2], Hua Jun Fan[2, *], Josh Daniel McLoud[1], Lizhi Ouyang[3], Zoe Brewer[1]

[1]Department of Chemistry, Science and Mathematics, Tabor College, Hillsboro, USA

[2]College of Chemical Engineering, Sichuan University of Science and Engineering, Zigong, PR China

[3]Department of Mathematical Sciences, Tennessee State University, Nashville, USA

Email address:

jamestitah@tabor.edu (James Tembei Titah), fanhuajun@suse.edu.cn (Hua Jun Fan)

[*]Corresponding author

To cite this article:

James Tembei Titah, Tara Sheets, Liang Yang, Hua Jun Fan, Josh Daniel McLoud, Lizhi Ouyang, Zoe Brewer. Comparative Analysis of the Experimental, Computational, and Bacterial Growth Inhibition Studies on the Structure of N-Salicylidene Alanine Ni (II) Complex. *Advances in Materials*. Vol. 10, No. 5, 2022, pp. 144-151. doi: 10.11648/j.sjc.20221005.12

Received: August 6, 2022; **Accepted**: August 25, 2022; **Published**: September 8, 2022

Abstract: The structure and binding mode of N-Salicylidene alanine Ni (II) Schiff-base complex has been analyzed using experimental and computational techniques. The synthesis, characterization and computational studies of the Schiff-base complex revealed a more stable square planar geometry (structure 4a). Characterization of the complex was done using melting point/decomposition temperatures, solubility test, FT-IR and UV-visible spectroscopy. The N-Salicylidene alanine Schiff-base complex was seen to have a different melting point from alanine, which was used in the synthesis. The complex was soluble in water and most polar solvents, which is important for its intended application in biological systems. In addition, IR spectra of the complex revealed prominent stretching frequencies including the -C=N- imine group that are similar within 5-10% margin to that of the most stable square planar computational model structure 4a. Furthermore, the UV-visible studies of the Schiff-base complex showed two prominent electronic transitions in both the experimental and computational model structures. These electronic transitions were assigned to the the $^3T_1 \rightarrow {}^3A_2$ and $^3T_1 \rightarrow {}^3T_2$ observed at 232 nm and 362 nm respectively. These transitions agree with the most stable square planar computational model structure corresponding to HOMO-6→LUMO+2, and HOMO→LUMO+1 observed at 236 nm and 372 nm respectively. Based on both the experimental and computational studies, the most stable structure of N-Salicylidene alanine Ni (II) Schiff-base complex adopts a square planar geometry around the Ni (II) center corresponding to structure 4a. The Schiff-base complex was found to be non-toxic towards prokaryotic gram positive (*Staphylococcus aureus, Staphylococcus epidermis, Streptococcus mutants*) and gram negative (*Aquaspirillum serpens Escherichia coli*) bacterial and eukaryotic (*Saccharomyces cerevisiae*) bacterial.

Keywords: Analysis, N-Salicylidene Alanine Ni (II), Experimental, Computational, Toxicity

1. Introduction

The study of Schiff-bases and their transition metal complexes is an ongoing process with substantial applications in biochemistry, bio-inorganic and medicinal chemistry. Previous research has shown that Schiff-base complexes contain potential binding sites to biomolecules that play essential roles in pharmacological processes and for use as drugs. In addition, Schiff-base complexes with transition metals have been shown to exhibit enhanced biological activities [1-8]. The presence of the imine (-C=N-) functional group in addition to the electronegative oxygen, nitrogen and/or sulfur donor atoms in transition metal Schiff-base complexes enhances their transportation across biological membranes. Furthermore, transition metal Schiff-base complexes have been used industrially as catalysts and exhibit a wide range of biological activities and/or properties such as

anti-fungal, anti-malarial, anti-bacterial, anti-diabetic, anti-cancer, anti-proliferative, anti-tumor, etc. There is ongoing research to design and develop new chemotherapeutic compounds from Schiff-bases derived from amino acids and their transition metal complexes for potential use in biochemistry, medicinal chemistry and/or drugs [9-15]. This publication will present a comparative analysis of the synthesis and preliminary characterization of N-Salicylidene Alanine Ni (II) complex, toxicity of the complex, and computational B3LYP density functional theory (DFT) studies on the structure of Ni (II) alanine Schiff-base complex by simulating the potential binding sites at the Ni (II) metal center.

Preliminary characterization of the complex will include melting/decomposition temperatures, solubility in different solvents, Fourier Transform Infra-red spectroscopy (FT-IR), and ultra violet-visible spectroscopy (UV-Vis). The computational DFT studies will compare the calculated results with the experimental results and predict the possible binding sites in the complex. In addition, the biological properties of the complex were assessed by determining its toxicity against a variety of bacterial cells. This is a very important consideration since this complex is intended to be used in biological systems with application as a drug.

2. Experimentation

2.1. General Synthetic Method

This is an in-situ synthesis. An equimolar amount of NaOH pellets and the amino acid were completely dissolved in a beaker using a suitable solvent (water, etc) with a magnetic stirrer at room temperature. An equimolar amount of the carbonyl compound was added drop-wise to the resulting solution while stirring continuously. The reaction was allowed to go on for about 45 minutes - 1 hour with stirring. A metal salt was added slowly in a 1:2 metal-ligand mole ratio and allowed to react for an additional 30 - 45 minutes with continuous stirring. The resulting solution was concentrated to approximately 50 - 60% of the original volume. The mixture was kept in the fume hood at room temperature. After 1 – 3 days, the resulting brightly colored crystals (powder) were filtered by suction, washed with cold solvent, air dried, and stored in well-protected vials. The percentage yield ranges from 60-85%.

2.1.1. Synthesis of N-Salicylidene Alanine Ni (II) Complex

Sodium hydroxide (0.0112 mols) and alanine (0.0112 mols) were dissolved in 30.0 mL of water in a 250 mL beaker while stirring continuously with the help of a magnetic stirrer at room temperature. An equimolar amount of salicylaldehyde (0.0112 mols) was added drop wise to the resulting mixture while stirring. The reaction was allowed to go on for 1 hour and a 30.0 mL aqueous solution of Nickel (II) Chloride ($NiCl_2$; 0.0061 mols) was slowly added onto the resulting solution and allowed to react for an additional 45 minutes in the fume hood. The resulting mixture was concentrated to 60% of the original volume to initiate crystallization. A bright green powder obtained was filtered through suction, air dried and stored in vials for subsequent characterization. The percentage yield was 85%.

All chemicals in this research were used as purchased without modification.

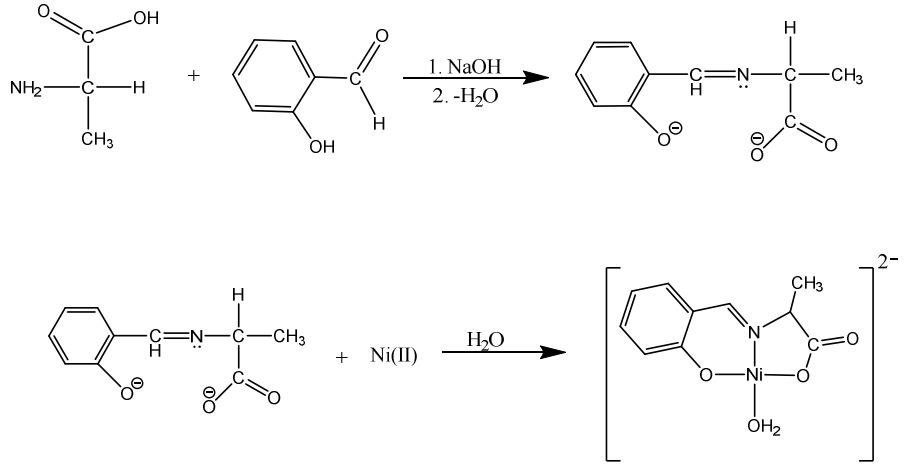

Figure 1. *Reaction scheme showing proposed structure for the Synthesis of N-Salicylidene Alanine Ni (II) Complex.*

2.1.2. Toxicity Test of N-Salicylidene Alanine Ni (II) Complex

The Kirby-Bauer assay was used to test our compound for bacterial growth against the following bacterial species: Aquaspirillum serpens, Escherichia coli strain K12, Saccharomyces cerevisiae strain Alpha 1, Staphylococcus aureus, Staphylococcus epidermis, and Streptococcus mutants. The Kirby-Bauer assay is the most sensitive test used for bacterial growth against prokaryotes and eukaryotes in microbiology [16-18].

In this paper, an aqueous solution of N-Salicylidene alanine (Ni (II) complex was prepared with a slightly higher antibiotic concentration (1μM) than those used in the Kirby-Bauer assay (30 μg). The antimicrobial and antimicrobial-free discs used in this research were purchased from Becton, Dickinson and Company located in New Jersey. The antimicrobial-free discs were placed in a sterile 2.0 mL

microcentrifuge tube containing the aqueous solution of the compound to be tested and centrifuged for 5 minutes at 12,000 x g to remove all air from the discs. The discs were stored at room temperature over night before being transferred to the culture plates. Each compound in the disk was placed greater than 24 mm apart, center to center, on the same 100 mm inoculated Mueller-Hinton culture plate. There were three culture plates of the same organism tested, these served as biological replicates in case there was inhibition of organism growth. The incubated plates were observed in log phase of growth to prevent bacteria with slower growth from skewing results [19].

2.2. Computational Method

The computational method used in this paper was the density functional theory technique B3LYP embedded in G09 with 6-31G (d, p) all electron basis set [20-22]. The structural geometries were fully optimized and all elements were analysed using this basis set with the exception of Nickel, which uses the LANL2DZ basis set for the valence electrons with the corresponding effective core potentials (ECPs). The lowest energy structure conformations were confirmed by separate frequency calculations using the same method and basis set [23-25]. The UV-Visible absorption spectra simulated using TD-DFT method and infrared (IR) spectra of these Ni-containing complexes were all modeled from the most stable conformation of the optimized structures [26, 27]. These calculated spectra of the different structural geometries would be compared to the experiment results to determine the potential binding modes of the alanine Schiff-base ligand to the Ni (II)-metal center. The geometric parameters (bond lengths and bond angles) of the most stable optimized structures are presented in Table A1 of the supporting materials.

3. Results and Discussion

3.1. Melting Point/Decomposition Temperature

Melting point/decomposition temperature is the basic and first characterization technique to differentiate between compounds. The melting point/decomposition temperature of the presumed N-Salicylidene Alanine Ni (II) complex was compared to the melting point of alanine using a melting point apparatus. The N-Salicylidene alanine Ni (II) complex melts at a temperature range of 210 - 212°C, which is different from the melting point range of alanine of 300 - 302°C indicates the synthesis of a new compound. The melting point of alanine agrees with the literature value [1, 2].

3.2. FT-IR Spectra of N-Salicylidene Alanine Ni (II) Complex

The FT-IR spectra of a solid sample of N-Salicylidene alanine Ni (II) complex was obtained using a FLUKA table top FT-IR instrument. Results of the prominent peaks are shown in table 2. The aromatic C-H stretch vibrates at from 3357 cm^{-1}, the C=O vibrates at 1625 cm^{-1}, while the imine (-C=N-) stretching shifts to 1520 cm^{-1}, the symmetric or asymmetric O-H vibrates at 3085 cm^{-1} and the aliphatic C-H stretch vibrates at 2951 cm^{-1}. This shift in stretching frequencies can be attributed to the bonding of these donor atoms to the Ni (II) center [1, 2]. The FT-IR spectra reveal that the proposed structure on N-Salicylidene alanine Ni (II) complex adopts a tetrahedral or square planar geometry.

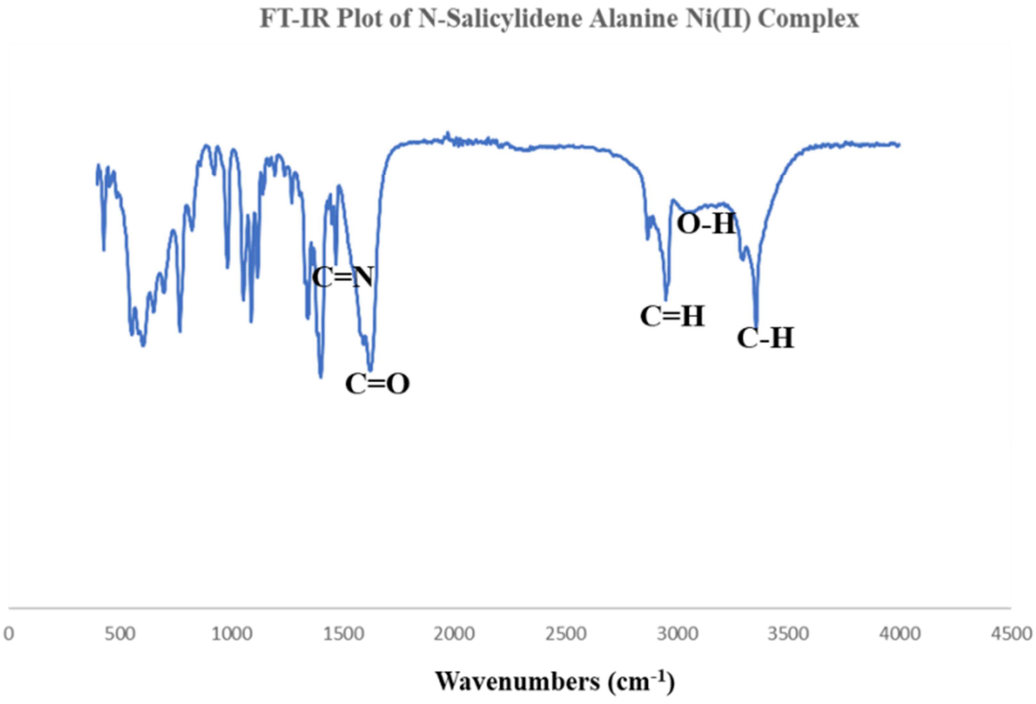

Figure 2. *FT-IR plot of N-Salicylidene Alanine Ni (II) Complex showing prominent peaks.*

Table 1. *IR vibration frequencies showing prominent peaks in the Ni (II) complex.*

IR stretching frequencies (cm^{-1})	Assignment
3299, 3357	Aromatic C-H stretching
3085	O-H (symmetric or asymmetric vibration of water)
1625	C=O stretching
1520	Imine (-C=N-) stretching
2951	Aliphatic C-H stretching

3.3. UV-Visible Spectroscopy and Energy Calculation

N-Salicylidene Alanine Ni (II) complex was pale blue, which implies that it can undergo electronic transition in both tetrahedral (square planar) and octahedral environments. The UV-visible spectra of our compound showed two prominent absorption peaks around 232 nm 362 nm, the middle weak peak absorbs at 276 nm (see figure 3).

These peaks can be assign to the $^3T_1 \rightarrow {}^3A_2$ and $^3T_1 \rightarrow {}^3T_2$ electronic transitions in the tetrahedral or square planar environment or $^3T_1g \rightarrow {}^3A_2g$ and $^3T_1g \rightarrow {}^3T_2g$ electronic transitions in the octahedral environment. The electronic transitions and energies are shown in Table 2. The electronic transition at 232 nm is more intense and absorbs at a higher energy (8.568 x 10^{-19} J) than the electronic transition at 362 nm (5.491 x 10^{-19} J).

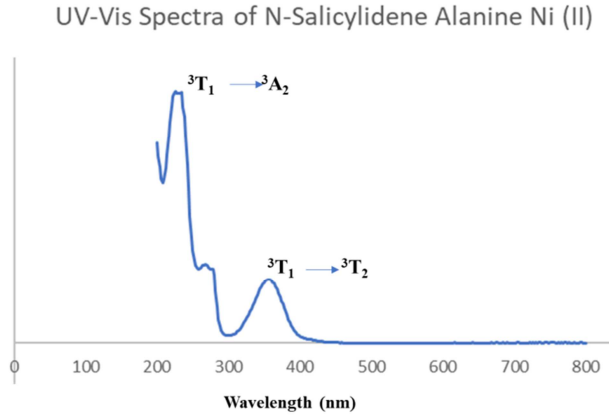

Figure 3. *UV-visible spectra showing the electronic transitions in the Ni (II) complex.*

Table 2. *Electronic transitions showing the maximum wavelength in N-Salicylidene Alanine Ni (II) Complex.*

Compound Colour	Max. wavelength (λ_{max}, nm)	Energy (x 10^{-19} J)	Transition
N-Salicylidene alanine Ni (II)	232	8.568	$^3T_1 \rightarrow {}^3A_2$
Green	362	5.491	$^3T_1 \rightarrow {}^3T_2$

3.4. Solubility on N-Salicylidene Alanine Ni (II) Complex

The solubility of our Ni (II) complex was determined in different solvents. This was done by dissolving approximately 0.100 g sample of the complex in approximately 10.00 mL of solvent. It is important to note that our complex is soluble in water and other polar solvents an insoluble in non-polar solvents. The solubility of the complex increases in the warm solvent. The increased solubility of our complex is paramount since it is intended to be used in biological systems. Results of the test are shown in table 3.

Table 3. *Solubility of N-Salicylidene Alanine in selected solvents.*

Compound/solvent	Water	Ethanol	methanol	chloroform	hexane	D_2O
N-Salicylidene alanine Ni (II)	s	s	ss	I	i	s

s = soluble; i = insoluble; ss = sparingly soluble.

4. Growth Inhibition Properties of N-Salicylidene Alanaine Ni (II) Complex

The Kirby-Bauer assay test was used to investigate the growth inhibition properties of our compound against bacterial cells-prokaryotes and a eukaryote. The bacterial cells used include: gram negative Aquaspirillum serpens and Escherichia coli, and gram-positive Staphylococcus aureus, Staphylococcus epidermis, and Streptococcus mutants. The results indicate that N-Salicylidene alanine Ni (II) complex was growth resistance or non-toxic against gram-negative, gram-positive and eukaryotic bacterial cells. The results including all replicates are shown in table 4.

Table 4. *Kirby-Bauer Susceptibility Test.*

Prokaryotes	N-Salicylidene Alanine Ni (II)	Positive control	Negative control
Gram negative			
Aquaspirillum serpens	R	S	R
Escherichia coli	R	S	R
Gram positive			
Staphylococcus aureus	R	S	R
Staphylococcus epidermis	R	S	R
Streptococcus mutants	R	S	R

Prokaryotes	N-Salicylidene Alanine Ni (II)	Positive control	Negative control
Eukaryote Saccharomyces cerevisiae	R	S	R

S = isolates were susceptible to growth, R = isolates were resistant to growth.

5. Computational Studies on N-Salicylidene Alanine Ni (II) Complex

Computational simulations were employed to investigate the binding environment of the alanine Schiff-base ligand and its possible binding modes to the Ni (II) center. Four Nickel-alanine Schiff-base structural models were proposed and the most stable geometries are shown in figure 4. We can see from figure 4 that Ni (II) prefers to adopt a square planar geometry. The ligand in models 4a and 4b contains deprotonated carboxylate group and deprotonated hydroxyl group while the ligand in models 4c and 4d contains only the deprotonated carboxylate group [28, 29]. All four structural models showed a square planar geometry around the Ni (II) center where three of the binding sites are from the ligand (N, carboxylate O, hydroxyl O), and the fourth binding site is from either water (4a and 4c) or Chlorine (4b and 4d).

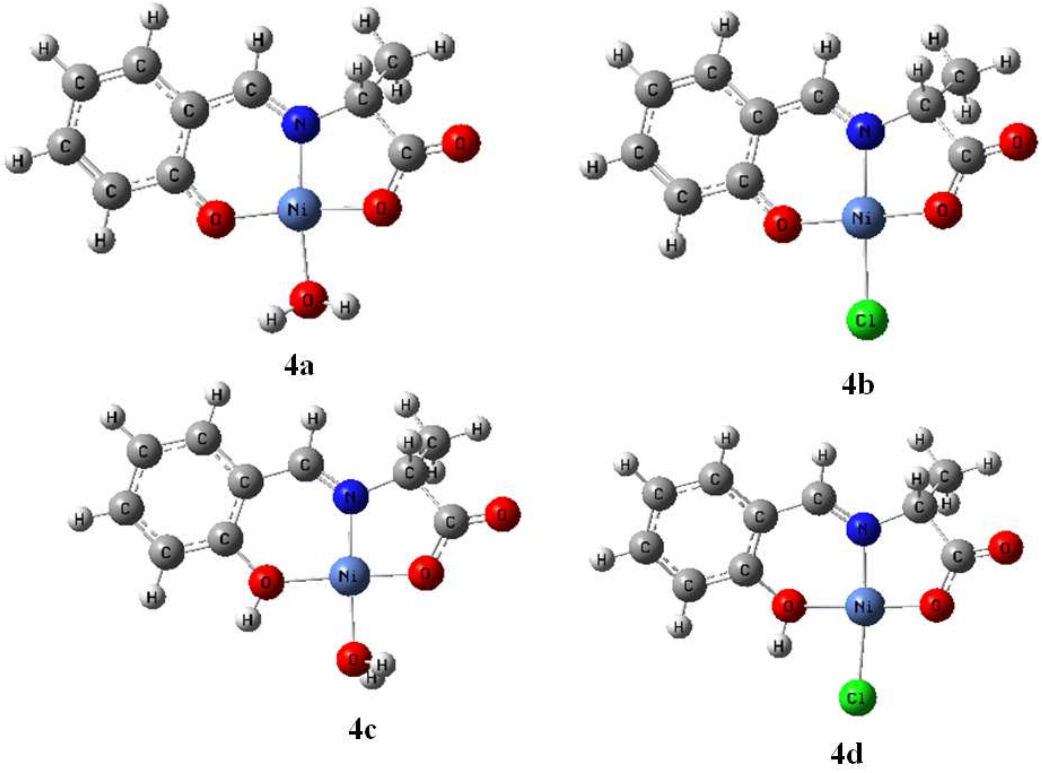

Figure 4. *Proposed structural geometries of four Ni (II)-alanine Schiff-base models.*

From Table A1 and figure 4, one can see that the Ni-N bond lengths were slightly elongated when Ni binds to a Cl^- ligand than to a H_2O ligand. For example, Ni-N bond length increases from 1.8387 Å in 4a to 1.8951 Å in 4b. A similar elongation is observed from 1.8577 Å in 4c to 1.8851 Å in 4d. This gives an elongation of 0.03 - 0.05 Å. The similar elongation in bond length of 0.03 – 0.04 Å was observed between Ni-O1 and Ni-O2. The elongation induced by the fourth ligand (water or chloride) on the rest of bond lengths between 4a *vs* 4b and 4c *vs* 4d models was insignificant.

The deprotonated hydroxyl groups of alanine Schiff-base also influences the bond lengths around the Ni (II) center greatly. For example, the bond length of Ni-O1 increases from 1.8305 Å in 4a (deprotonated) to 1.9430 Å in 4c (protonated), and 1.8722 Å in 4b (deprotonated) to 1.9462 Å in 4d (protonated). Furthermore, the O-H bond length of phenol group increases by 0.09 Å in 4c and 4d. This might be due to the fact that the hydrogen on the hydroxyl group weakens its oxygen (O) binding ability to the Ni (II) center. Correspondingly, the opposite Ni-O2 bond lengths were shortened by 0.05 Å in 4c and 4d.

Interestingly, the square planar geometries at the Ni (II) center were slightly distorted. For example, the N-Ni-O1 bond angles were 97.6°, 93.5°, 94.1°, 91.1° and N-Ni-O2 bond angles 87.9°, 85.7°, 88.3°, 87.5° for 4a – 4d respectively. This is probably due to the formation of the six-member ring on the left side *vs* the five-member ring on the right side. As such the N-Ni-O4 bond angles were 173.4° (4a) and 176.2° (4c), and N-Ni-Cl bond angles were 176.8° (4b) and 173.9° (4d), respectively.

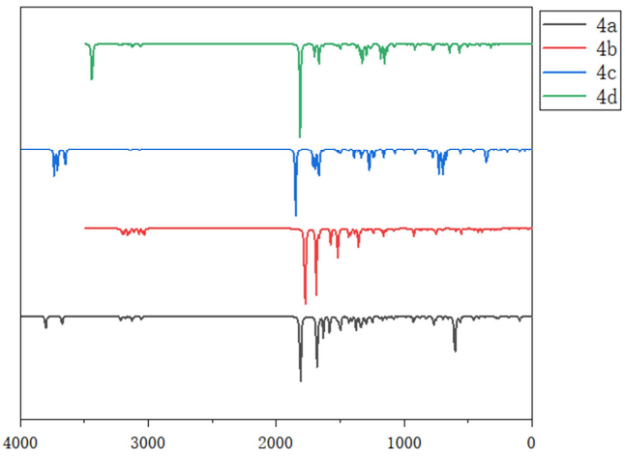

Figure 5. *The calculated IR spectra of the model structures 4a - 4d.*

The calculated IR spectra of structures 4a – 4d are shown in figure 5. When compared with the experimental IR spectra of N-Salicylidene alanine Ni (II) complex (figure 2), we can see the profile of calculated IR spectra of 4a resembles closely with the experimental spectra. By examining the stretching mode of these peaks, the peak at 1811 cm^{-1} was assigned to the stretching of carbonyl (C=O) group, the peak 1682 cm^{-1} was assigned to the imine (-C=N-) functional group, and the peaks 603 and 1581 cm^{-1} were assigned to the rocking vibration modes of water. Various peaks around 3000 - 3800 cm^{-1} were assigned to symmetric or asymmetric vibration of water or hydroxyl groups [30, 31]. While the absolute values of the calculated IR peaks differ slightly, the peak profile at 600, 1700 and 3700 cm^{-1} regions match well with the experiment results.

Figure 6 shows the calculated UV-visible spectra of model structures 4a – 4d. We can observe that the calculated spectra profile of 4a matches well with the experiment results. The prominent peaks predicted were shown at 239 nm, 284 nm, and 372 nm. The corresponding transition occurred mainly at HOMO-6→LUMO+2, HOMO-1→LUMO+2, and HOMO→LUMO+1. Based on these modeling results, the most probable structure would be 4a.

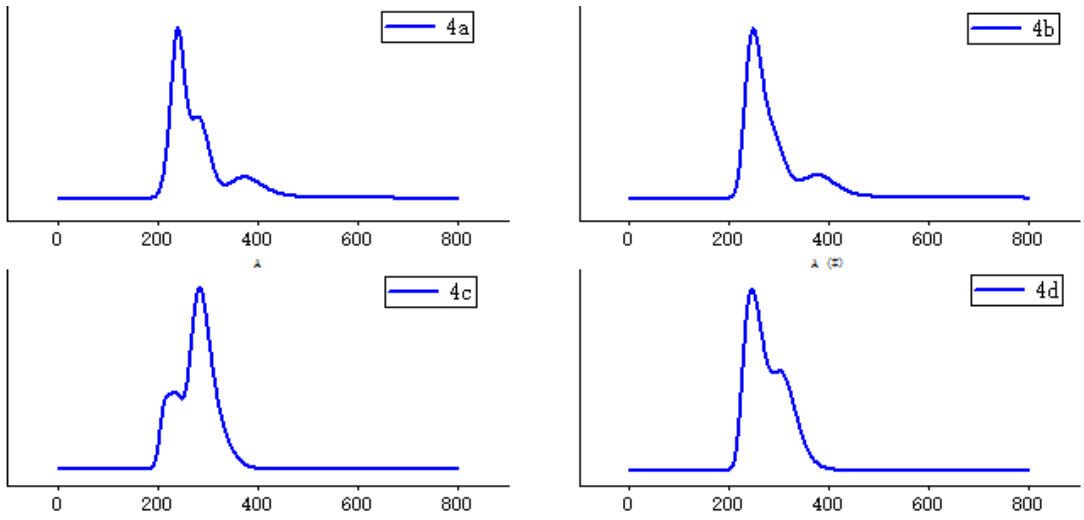

Figure 6. *The calculated UV-vis spectra of model structures 4a - 4d.*

6. Conclusion

We have successfully synthesized and characterize the Ni (II) Schiff-base complex derived from alanine; N-Salicylidene Alanine Ni (II) supported with computational results. The melting point/decomposition temperature of our complex was different from the melting point of alanine, which was the starting amino acid. This is a simple chemical technique to confirm that a new compound was synthesized. In addition, the compound was seen to dissolve in water and other polar solvents tested. This is an important aspect about the complex since it is required to be used in biological systems. The FT-IR and UV-visible spectra reveal prominent vibrational peaks and electronic transitions that agrees with computational results and literature. Most of the stretching frequencies in the complex were shifted due to binding to the central Ni (II) center and the two prominent electronic transitions were assigned to $^3T_1 \rightarrow {}^3A_2$ and $^3T_1 \rightarrow {}^3T_2$ observed at 232 nm and 362 nm respectively. These transitions agree with the calculated transitions HOMO-6→LUMO+2 and HOMO→LUMO+1. Furthermore, the IR spectra of the experimental structure resembles the calculated IR spectra of the most stable square planar model structure 4a. The binding sites on the ligand are on the nitrogen, carboxylate oxygen, and hydroxyl oxygen atoms with the fourth binding site on the oxygen atom of water ligand. Finally, our complex was found to be non-toxic towards prokaryotic gram positive (Staphylococcus aureus, Staphylococcus epidermis, Streptococcus mutants) and gram negative (Aquaspirillum serpens Escherichia coli) bacterial and eukaryotic (Saccharomyces cerevisiae) bacterial.

Acknowledgements

We are highly indebted to Tabor College for providing the

laboratory space and chemicals used in this research.

We thank Dr. James Bann, Department of Chemistry at Wichita State University for providing access in the IR, and UV-visible instruments used for the characterization of our compounds.

We also give thanks to the High-Performance Computing Center at the Sichuan University of Science and Engineering for the computational resources used in this research. Partial financial support comes from Science Foundation of Sichuan University of Science & Engineering (2020RC06) and Sichuan Provincial Natural Science Foundation (SYZ202133 & 22RCYJ0029).

Appendix

Table A1. *The geometric parameters (bond lengths and bond angles) of the most stable optimized structures (4a-4d).*

	4a	4b	4c	4d
Ni-N1	1.8387	1.8951	1.8577	1.8851
Ni-O1	1.8305	1.8722	1.9430	1.9462
Ni-O2	1.8361	1.8682	1.7865	1.8133
Ni-O4	1.9659		1.9653	
Ni-Cl		2.2407		2.2205
C1-C2	1.4207	1.4324	1.3870	1.3914
C1-C6	1.4351	1.4400	1.4089	1.4110
C1-O1	1.3066	1.2885	1.3923	1.3752
C2-C3	1.3817	1.3790	1.3970	1.3951
C2-H1	1.0873	1.0859	1.0873	1.0864
C3-C4	1.4112	1.4143	1.3976	1.3979
C3-H2	1.0873	1.0889	1.0853	1.0858
C4-C5	1.3790	1.3805	1.3886	1.3897
C4-H3	1.0853	1.0865	1.0845	1.0850
C5-C6	1.4182	1.4156	1.4118	1.4081
C5-H4	1.0882	1.0899	1.0863	1.0869
C6-C7	1.4302	1.4301	1.4507	1.4585
C7-H5	1.0938	1.0968	1.0925	1.0944
C7-N1	1.2976	1.2956	1.2900	1.2862
C8-H6	1.0979	1.0991	1.0967	1.0967
C8-N1	1.4757	1.4678	1.4858	1.4719
C8-H6	1.0979	1.0991	1.0967	1.0967
C8-C9	1.5343	1.5350	1.5344	1.5354
C9-H7	1.0954	1.0970	1.0944	1.0958
C9-H8	1.0953	1.0958	1.0948	1.0957
C9-H9	1.0932	1.0937	1.0931	1.0931
C8-C10	1.5441	1.5446	1.5359	1.5451
C10-O2	1.3163	1.2961	1.3366	1.3146
C10-O3	1.2168	1.2288	1.2055	1.2158
O4-H10	0.9717		0.9765	
O4-H11	0.9754		0.9788	
O1-H12			0.9739	0.9883
C1-O1-Ni	126.23	128.14	128.57	126.71
O1-Ni-N1	97.62	93.58	94.09	91.11
O2-Ni-N1	87.94	85.65	88.27	87.49
O1-Ni-Cl		89.56		83.88
O1-Ni-04	88.92		89.70	
O2-Ni-04	85.58		87.91	
O2-Ni-Cl		91.23		97.58
O1-Ni-O2	173.36	178.01	176.98	178.28
N1-Ni-O4	173.41		176.15	
N1-Ni-Cl		176.80		173.9
Ni-O2-C10	116.31	117.52	117.22	116.61

References

[1] James T. Titah, Coulibaly W. Karime, Kevin Chambers, Anita Balogh, Kevin Joannou. Synthesis, Characterization and Bacterial Growth Inhibitory Properties of Schiff-Base Ligands Derived from Amino Acids. Science Journal of Chemistry, 2020, Vol. 8, (1), pp 1-6.

[2] Abu-Dief A. M., and Mohamed I. M. A. Beni-Suef University Journal of Basic and Applied Sciences, 2015, (4), pp 119-133; Helmut Quast, Wolfgang Nüdling, Gerhard Klemm, Andreas Kirschfeld, Patrik Neuhaus, Wolfram Sander, David A. Hrovat and Weston Thatcher Borden. A Perimidine-Derived Non-Kekulé Triplet Diradical. The Journal of Organic Chemistry, 2008, Vol. 73, (13), pp 4956-4961. https://doi.org/10.1021/jo800589y

[3] Ghosh K. et al., RSC Advances, 2018, (8), pp 28216-28237.

[4] Mohamed Gaber et al., Journal of Iranian Chemical Society, 2019, (16), pp 169-182, b. M. Alias, H. Kassum and C. Shakir, JAAUBAS, 2014, Vol. 15, pp 28-34.

[5] Kangah Niameke Jean-Baptiste et al., International Journal of Pharmaceutical Science Invention, 2019, (8), issue II, pp 48-54.

[6] Jawoor, S. S., Patil, S. A., & Toragalmath, S. S. Synthesis and characterization of heteroleptic schiff base transition metal complexes: a study of anticancer, antimicrobial, dna cleavage and anti-tb activity. Journal of Coordination Chemistry, 2018, Vol. 71, (2), pp 271–283.

[7] Chaudhary N. K. and Mishra P., bioinorganic chemistry and applications, 2017, pp 1-13.

[8] Emad Yousif et al., Arabian Journal of Chemistry, 2017, (10), pp S1639-S1644.

[9] Majid Rezaeivala, Journal of Saudi Chemical Society, 2017, (21), pp 420-424.

[10] Eliene Leandrode Araujo et al., International Journal of Biological Macromolecules, 2017, (95), pp 168-176.

[11] Mangamamba T., Ganorkar M. C., Swarnabala G., International Journal of Inorganic Chemistry, 2014, pp 1-22.

[12] El-Sherif A. A., Aljahdali M. S., Journal of Coordination Chemistry, 2013, Vol. 66, (19), pp 3423-3468.

[13] Rimbu C., Danac R., Pui A., Chem Pharm Bull., 2014, Vol. 62, (1), pp 12-15.

[14] Miessler G. L., Fisher P. J., and Tarr D. A., Inorganic Chemistry, 2013, 5th Edition.

[15] Kashyap, S., Kumar, S., Ramasamy, K. et al. Synthesis, biological evaluation and corrosion inhibition studies of transition metal complexes of Schiff base. Chemistry Central Journal, 2018, Vol. 12, pp 117.

[16] Bauer, A. W., Perry D. M., and Kirby W. M. M., Single disc antibiotic sensitivity testing of Staphylococci. A. M. A. Arch. Intern. Med. 1959, Vol. 104, pp 208–216.

[17] Bauer, A. W., Kirby W. M. M., Sherris J. C., and Turck M., Antibiotic susceptibility testing by a standardized single disk method. Am. J. Clin. Pathol. 1966, Vol., pp 36: 493-496.

[18] Kourmouli, A., Valenti, M., van Rijn, E., Beaumont, H., Kalantzi, O. I., Schmidt-Ott, A., & Biskos, G., Can disc diffusion susceptibility tests assess the antimicrobial activity of engineered nanoparticles. Journal of nanoparticle research: an interdisciplinary forum for nanoscale science and technology, 2018, Vol. 20, (3), pp 62. https://doi.org/10.1007/s11051-018-4152-3

[19] Hudzicki, J., Kirby-Bauer disk diffusion susceptibility test protocol. American society for microbiology, 2009, Vol. 15, pp 55-63.

[20] Tirado-Rives J. and Jorgensen W. L., "Performance of B3LYP density functional methods for a large set of organic molecules," J. Chem. Theory and Comput., 2008, Vol. 4, pp 297-306.

[21] Woon D. E. and Dunning Jr T. H., "Gaussian-basis sets for use in correlated molecular calculations. 3. The atoms aluminum through argon," J. Chem. Phys., 1993, Vol. 98 pp 1358-71.

[22] Rassolov V. A., Ratner M, A, Pople J. A., Redfern P. C., and Curtiss L. A., "6-31G* Basis Set for Third-Row Atoms," J. Comp. Chem., 2001, Vol. 22, pp 976-84.

[23] Parr R. G. and Yang W., Density-functional theory of atoms and molecules, 1989, Oxford Univ. Press, Oxford.

[24] Dobbs K. D. and Hehre W. J., "Molecular-orbital theory of the properties of inorganic and organometallic compounds. 4. Extended basis-sets for 3rd row and 4th row, main-group elements," J. Comp. Chem., 1986, Vol. 7, pp 359-78.

[25] De Castro E. V. R. and Jorge F. E., "Accurate universal gaussian basis set for all atoms of the periodic table," 1998, pp 5225-29.

[26] Adamo C., Le Bahers T., Savarese M., Wilbraham L., García G., Fukuda R., Ehara M., Rega N., and Ciofini I., "Exploring excited states using Time Dependent Density Functional Theory and density-based indexes," 2015, pp 166–178.

[27] Adamo C. and Jacquemin D., "The calculations of excited-state properties with Time-Dependent Density Functional Theory," 2013, pp 845.

[28] Wedig U., Dolg M., Stoll H., and Preuss H., in Quantum Chemistry: The Challenge of Transition Metals and Coordination Chemistry, Ed. A. Veillard, Reidel, and Dordrecht, 1986, pp 79.

[29] Schlegel H. B. and Frisch M. J., in Theoretical and Computational Models for Organic Chemistry, Ed. J. S. Formosinho, I. G. Csizmadia, and L. G. Arnaut, NATO-ASI Series C, Kluwer Academic, The Netherlands, 1991, Vol. 339, pp 5-33.

[30] Yamaguchi Y., Frisch M. J., Gaw J., Schaefer III H. F., and Binkley J. S., "Analytic computation and basis set dependence of Intensities of Infrared Spectra," J. Chem. Phys., 1986, Vol. 84, pp 2262-78.

[31] Barone V., Bloino J., Biczysko M., and Santoro F., "Fully integrated approach to compute vibrationally resolved optical spectra: From small molecules to macrosystems," J. Chem. Theory and Comput., 2009, Vol. 5, pp 540-54.